ADVANCED FUNCTIONAL MATERIALS
www.afm-journal.de

Organic–Inorganic Hierarchical Self-Assembly into Robust Luminescent Supramolecular Hydrogel

*Zhiqiang Li, Zhaohui Hou, Hongxian Fan, and Huanrong Li**

Luminescent hydrogels are of great potential for many fields, particularly serving as biomaterials ranging from fluorescent sensors to bioimaging agents. Here, robust luminescent hydrogels are reported using lanthanide complexes as emitting sources via a hierarchical organic–inorganic self-assembling strategy. A new organic ligand is synthesized, consisting of a terpyridine unit and two flexibly linked methylimidazole moieties to coordinate with europium(III) (Eu^{3+}) tri-thenoyltrifluoroacetone ($Eu(TTA)_3$), leading to a stable amphiphilic Eu^{3+}-containing monomer. Synergistic coordination of TTA and terpyridine units allows the monomer to self-assemble into spherical micelles in water, thus maintaining the luminescence of Ln complexes in water. The micelles further coassemble with exfoliated Laponite nanosheets coated with sodium polyacrylate into networks based on the electrostatic interactions, resulting in the supramolecular hydrogel possessing strong luminescence, extraordinary mechanical property, as well as self-healing ability. The results demonstrate that hierarchical organic–inorganic self-assembly is a versatile and effective strategy to create luminescent hydrogels containing lanthanide complexes, giving rise to great potential applications as a soft material.

1. Introduction

Luminescent organogels containing organic dyes, quantum dots, or metal complexes as emitting sources have attracted broad attention due to their unique optical properties and functional versatility.[1] Particularly, due to their functional versatility and synthetic simplicity, luminescent organogels employing metal complexes as the emitting sources have shown great potential applications in fluorescent sensors, bioimaging agents, display and light devices, and electrophotonic devices.[2] In principle, incorporation of lanthanide (Ln) complexes into matrices, such as polymers and ionic liquids, allows for creation of luminescent organogels exhibiting narrow, tunable emission bands and long radiative lifetimes.[3] However, preparation of such luminescent hydrogels possessing extraordinary photophysical and mechanical properties along with self-healing feature still remains challenging.[4] On the one hand, the excited state of Ln complexes can be significantly quenched by water through the excitation of O—H vibrations.[5] On the other hand, the mechanical properties of supramolecular gels typically suffer from the relatively weak noncovalent interactions among the constituent components.[6] This drawback also limits construction of free-standing objects from the luminescent gels.[7] Herein for the first time, we report on robust, self-healable luminescent hydrogels based on the self-assembly of metal–organic complexes and inorganic components into hierarchical nanostructures driven by metal coordination and electrostatic interactions.

To address the problem of luminescence quenching in hydrogels, we designed and synthesized one functional organic ligand consisting of a terpyridine moiety and two flexibly linked 3-methylimidazolium bromide units (tpy-mim_2). In our study, exfoliated Laponite nanosheets coated with sodium polyacrylate (ASAP) was employed as the inorganic components to improve the mechanical property of hydrogels,[8] while europium(III) (Eu^{3+}) tri-thenoyltrifluoroacetone ($Eu(TTA)_3$) was utilized as the emission precursor whose luminescence is usually quenched in the presence of ASAP.[9] Coordinating the precursor with the terpyridine moiety of ligand tpy-mim_2 led to formation of an stable amphiphilic monomer $Eu(TTA)_3$tpy-mim_2 by overcoming the competitive coordination of ASAP and water. This amphiphilic monomer self-assembled into supramolecular micelles in water where the Eu^{3+} complexes were buried in hydrophobic microenvironment, thus maintaining the luminescence of Eu^{3+} ions and rendering the hydrogels radiative with a long lifetime. Association of Laponite nanosheets coated with oxyanions with the imidazolium salts on the surface of the supramolecular assemblies via electrostatic interactions resulted in formation of robust luminescent hydrogels (**Scheme 1**).[8a,10] It is worth noting that the surrounding rich noncovalent interactions among different components within the hybrid organic–inorganic hierarchical hydrogels give rise to their rapidly and quantitatively self-healing property.

2. Results and Discussion

Ligand tpy-mim_2 was synthesized by a four-step procedure and comprehensively characterized, while the $Eu(TTA)_3$

Dr. Z. Li, Z. Hou, H. Fan, Prof. Dr. H. Li
School of Chemical Engineering and Technology
Hebei University of Technology
GuangRong Dao 8, Hongqiao District
Tianjin 300130, P. R. China
E-mail: lihuanrong@hebut.edu.cn

DOI: 10.1002/adfm.201604379

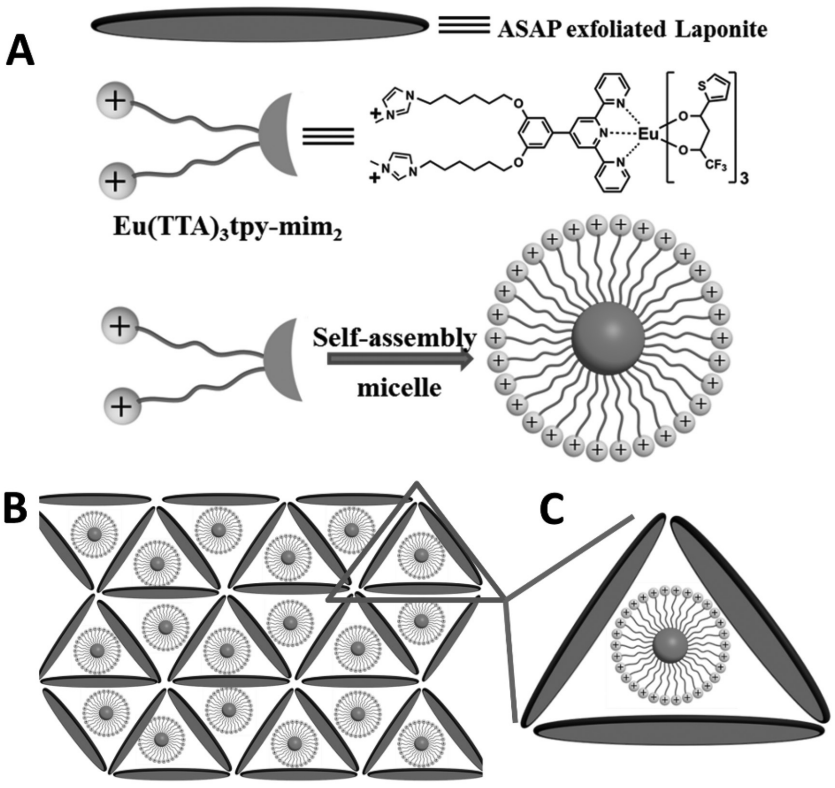

Scheme 1. A) Graphical representation of ASAP exfoliated Laponite, chemical structure of **Eu(TTA)$_3$tpy-mim$_2$** complexes, and the schematic illustration of the micelles formed by **Eu(TTA)$_3$tpy-mim$_2$** complexes. B) Proposed structures for the formed supramolecular hydrogels from the micelles and the ASPA exfoliated Laponite nanosheets, where C) a magnified subunit of the supramolecular hydrogels was shown.

was prepared according to a reported method.[11] The lanthanide-containing amphiphilic monomer **Eu(TTA)$_3$tpy-mim$_2$** (**Scheme 2**) was prepared straightforwardly by coordination of tpy-mim$_2$ with Eu(TTA)$_3$ in MeOH and fully characterized with regard to its chemical structure and purity by ^{1}H nuclear magnetic resonance (NMR) spectroscopy, electrospray ionization mass spectroscopy, and elemental analysis (Figures S1–S11, Supporting Information).

We initially characterized the photoluminescent property of **Eu(TTA)$_3$tpy-mim$_2$** and its counterparts in both the solid state and solution. As shown in **Figure 1**, while Eu(TTA)$_3$ (Figure 1A(iii)) exhibited the typical characteristic color and brightness of Eu(III) complexes upon irradiation at 365 nm light, a more intensive luminescence of **Eu(TTA)$_3$tpy-min$_2$** compared to that of Eu(TTA)$_3$ was observed (Figure 1A(i)). Improvement of the brightness of **Eu(TTA)$_3$tpy-min$_2$** could be potentially attributed to the successful coordination of Eu^{3+} with ligand tpy-mim$_2$. To confirm this hypothesis, we synthesized another compound Eu(TTA)$_3$tpy that possesses the same coordination mode with **Eu(TTA)$_3$tpy-mim$_2$**, while lacking the alkyl tail-connected imidazole units. In the solid state, Eu(TTA)$_3$tpy displayed a comparable luminescence intensity to that of **Eu(TTA)$_3$tpy-mim$_2$** (Figure 1A(ii) and the blue line in Figure 1B). This indicates that coordination of Eu^{3+} ions with terpyridine and TTA units synergistically results in their strong luminescence.

We subsequently investigated the photoluminescent properties of solid-state **Eu(TTA)$_3$tpy-mim$_2$** and its counterparts by probing the $^5D_0 \rightarrow {}^7F_2$ transition (Figure 1B). The excitation spectrum of Eu(TTA)$_3$ showed a broad band in the range of 240–450 nm ascribed to the absorption of TTA ligand, suggesting occurrence of the ligand (TTA) to metal (Eu^{3+}) energy transfer.[12] Coordinating Eu(TTA)$_3$ with ligands tpy-mim$_2$ or terpyridine led to an intensive characteristic excitation for both TTA and terpyridine units, suggesting the synergistically cochelating effect on efficiently exciting Eu^{3+} ions. These results directly support the formation of **Eu(TTA)$_3$tpy-min$_2$** and Eu(TTA)$_3$tpy based on the complexation between precursor Eu(TTA)$_3$ and the terpyridine moiety, thus leading to ternary lanthanide complexes.[13] In addition, the emission spectrum of Eu(TTA)$_3$ (the black line in Figure 1B), Eu(TTA)$_3$tpy (the blue line in Figure 1B), and **Eu(TTA)$_3$tpy-mim$_2$** (the red line in Figure 1B) powder displayed five sharp peaks at 579, 592, 614, 650, and 698 nm, which could be assigned to the $^5D_0 \rightarrow {}^7F_J$ (J = 0–4) transitions. Among the peaks, the $^5D_0 \rightarrow {}^7F_2$ band at 614 nm is predominantly responsible for the luminescence emission in red. Compared to precursor Eu(TTA)$_3$, an enhanced luminescence intensity for the coligand system **Eu(TTA)$_3$tpy-mim$_2$** and Eu(TTA)$_3$tpy was observed. Fitting the photoluminescent emission decay curves to a monoexponential function yields the decay time of the photoluminescence of Eu(TTA)$_3$, Eu(TTA)$_3$tpy, and **Eu(TTA)$_3$tpy-min$_2$** to be 0.371, 0.604, and 0.652 ms, respectively (Figures S13–S15, Supporting Information). These results demonstrate that the luminescent property of solid Eu^{3+} complexes is significantly improved by chelating Eu^{3+} ions with TTA and terpyridine units synergistically (**Table 1** and Table S1 (Supporting Information)).

We also probed the photoluminescent features of Eu(TTA)$_3$ (Figure 1A(vi)), Eu(TTA)$_3$tpy (Figure 1A(v)), and **Eu(TTA)$_3$tpy-mim$_2$** (Figure 1A(iv)) in aqueous solution. Interestingly, we found that the strong luminescence of **Eu(TTA)$_3$tpy-mim$_2$** in water was maintained, while dissolving Eu(TTA)$_3$ and Eu(TTA)$_3$tpy in aqueous solution led to a dramatic decrease of their luminescence (due to the lack of imidazolium salt, Eu(TTA)$_3$ and Eu(TTA)$_3$tpy are not soluble in neat water, we chose mixed solvent EtOH/H_2O, v:v = 1:9 instead). Although Eu(TTA)$_3$tpy has the same coordination parameters with **Eu(TTA)$_3$tpy-mim$_2$**, the presence of water molecules leads to obvious luminescent quenching. These results suggest that synergistically coordinating TTA and tpy-min$_2$ units with Eu^{3+} ions enables the retaining of the luminescence of Ln complexes in the aqueous phase by shielding them from water molecules and avoiding the luminescence quench of the complexes caused by the strong Eu^{3+}-OH coordination.

Adv. Funct. Mater. **2016**,
DOI: 10.1002/adfm.201604379

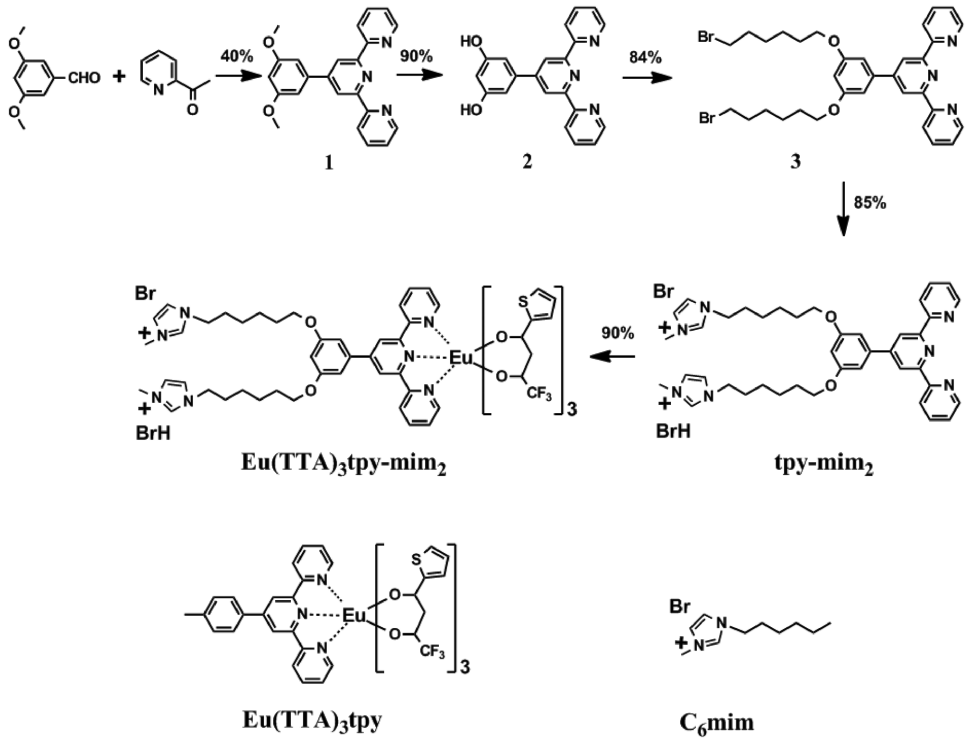

Scheme 2. The synthetic routes of amphiphilic monomer **Eu(TTA)$_3$tpy-mim$_2$**, chemical structure of Eu(TTA)$_3$tpy and C$_6$mim.

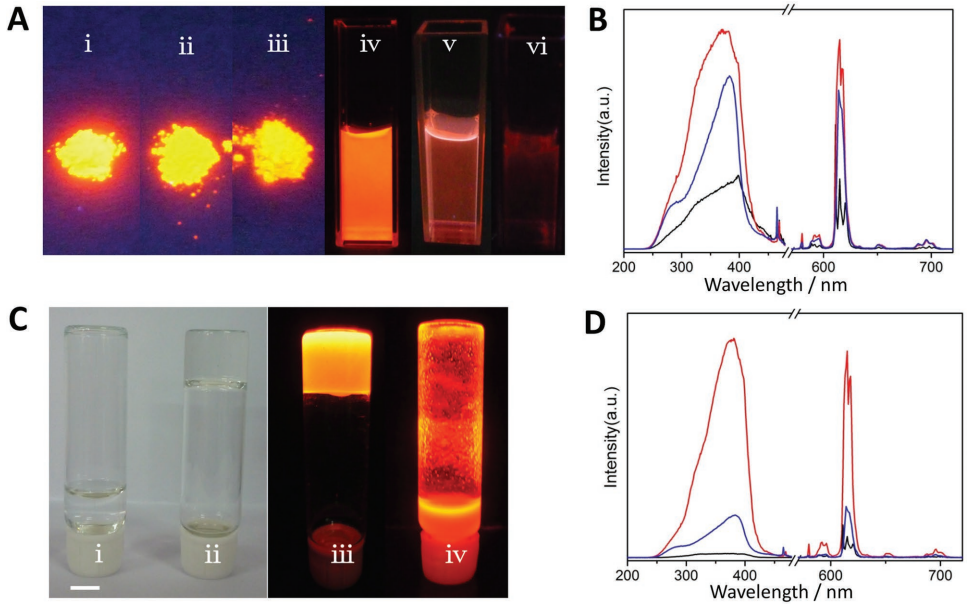

Figure 1. Optical properties. A) Digital photos of (i, iv) **Eu(TTA)$_3$tpy-mim$_2$**, (ii, v) Eu(TTA)$_3$tpy, and (iii, vi) Eu(TTA)$_3$ in solid state and in solution upon exposure to UV light (365 nm). While Eu(TTA)$_3$tpy and Eu(TTA)$_3$ were dissolved in mixed ethanol and water (EtOH/H_2O, v:v = 1:9), **Eu(TTA)$_3$tpy-mim$_2$** was dissolved in neat water. The concentration of the solutions was 0.5 mmol L^{-1}. B) Excitation (left) and emission (right) luminescence spectra of the powder Eu(TTA)$_3$ (black), Eu(TTA)$_3$tpy (blue), and **Eu(TTA)$_3$tpy-mim$_2$** (red). (λ_{ex} = 380 nm). C) Hydrogelation by mixing ASAP exfoliated Laponite and **Eu(TTA)$_3$tpy-mim$_2$** micellar binder in water. Pictures of (i)Laponite/ASAP/ **Eu(TTA)$_3$tpy-mim$_2$** = 2.9/0.087/0 wt%; Laponite/ASAP/ **Eu(TTA)$_3$tpy-mim$_2$** = 2.9/0.087/0.077 wt% ([**Eu(TTA)$_3$tpy-mim$_2$**] = 0.5 mmol L^{-1}) under (ii) daylight and (iii) 365 nm UV lamp illumination. (iv) Supramolecular hydrogels after addition of C$_6$mim. (The scale bar is 1 cm). D) Excitation (left) and emission (right) luminescence spectra of the supramolecular hydrogel (red) and physical mixture of Eu(TTA)$_3$tpy (blue) or Eu(TTA)$_3$ (black) water suspension with ASAP exfoliated Laponite at the same Eu^{3+} concentration. (λ_{ex} = 380 nm).

Table 1. Luminescence lifetime τ and the number of water molecules coordinated to Eu^{3+}.

Sample	τ_H [ms]	τ_D [ms]	q
$Eu(TTA)_3$tpy-mim_2 dissolved in	0.542	0.652	0.07
$Eu(TTA)_3$tpy dispersed in	0.413	0.604	0.61
$Eu(TTA)_3$ dispersed in	0.221	0.371	1.93
Supramolecular hydrogel	0.524	0.625	–
Physical mixture of $Eu(TTA)_3$tpy water suspension with ASAP exfoliated Laponite	0.271	0.339	–
Physical mixture of $Eu(TTA)_3$ water suspension with ASAP exfoliated Laponite	0.108	0.115	–

To gain insight into the mechanism of retaining strong luminescence of Eu^{3+} ions in water, we further characterized the assembling behavior of the amphiphilic monomer **$Eu(TTA)_3$tpy-mim_2** in water by transmission electron microscopy (TEM), scanning electron microscopy (SEM), and dynamic light scattering (DLS). Conventional TEM showed formation of uniform spherical micelles by **$Eu(TTA)_3$tpy-min_2** in water with an average diameter of 27 nm (**Figure 2**A). DLS determined the average hydrodynamic radius (R_h) of the assemblies to be 30.4 nm with a narrow distribution (Figure 2B), which is comparable with that obtained from the TEM experiment. In addition, the ratio R_g/R_h (R_g: gyration radius) was calculated to be 0.79 based on a reported reference method,[14] which is a characteristic feature for spherical micelles ($R_g/R_h < 1$). This result confirms the formation of spherical micelles by **$Eu(TTA)_3$tpy-mim_2** in water. We proposed that monomer **$Eu(TTA)_3$tpy-mim_2** formed spherical micelles in water, where the Eu^{3+} complexes are localized within the hydrophobic core of the micelles and positively charged imidazolium salts cover their surface. Hence, the extraordinary luminescent properties of micellar **$Eu(TTA)_3$tpy-mim_2** in water can be attributed to two facts. On one hand, synergistic coordination of Eu^{3+} with TTA and terpyridine units increases the coordination number of Eu^{3+} ions. This increase of the coordination number physically shields Eu^{3+} ions from water.[4b] On the other hand, formation of spherical micelles by the monomer creates a hydrophobic microenvironment for Eu^{3+} ions within the assemblies, thus preventing diffusion of water molecules to Eu^{3+} complexes. Overall, our results clearly demonstrate the luminescent property of Eu^{3+} complexes can be maintained in water by synergistically chelating with TTA and tpy-mim_2.

To verify our hypothesis on shielding the Eu^{3+} complexes from water in spherical micelles, the number of water molecules in the first coordination sphere of Eu^{3+} ions in **$Eu(TTA)_3$tpy-mim_2**, $Eu(TTA)_3$tpy, and $Eu(TTA)_3$ can be estimated by using the following equation[15]

$$q = 1.2(\tau_H^{-1} - \tau_D^{-1} - 0.25) \quad (1)$$

Where q represents the coordinated water molecules, and τ_H and τ_D is the luminescence lifetime measured in H_2O and D_2O, respectively. The luminescence lifetime of $Eu(TTA)_3$ dispersed in H_2O decreased significantly compared to that observed in the D_2O medium (Table 1). Based on these values, the coordinated water number q in $Eu(TTA)_3$ was determined as 1.93, indicating that almost two water molecules coordinate to Eu^{3+} ions in the $Eu(TTA)_3$ complexes.[16] Although synergistically coordinating with TTA and tpy units, the coordinated water number of $Eu(TTA)_3$tpy was determined to be 0.61, leading to an obvious luminescence lifetime decrease in H_2O (Table S1,

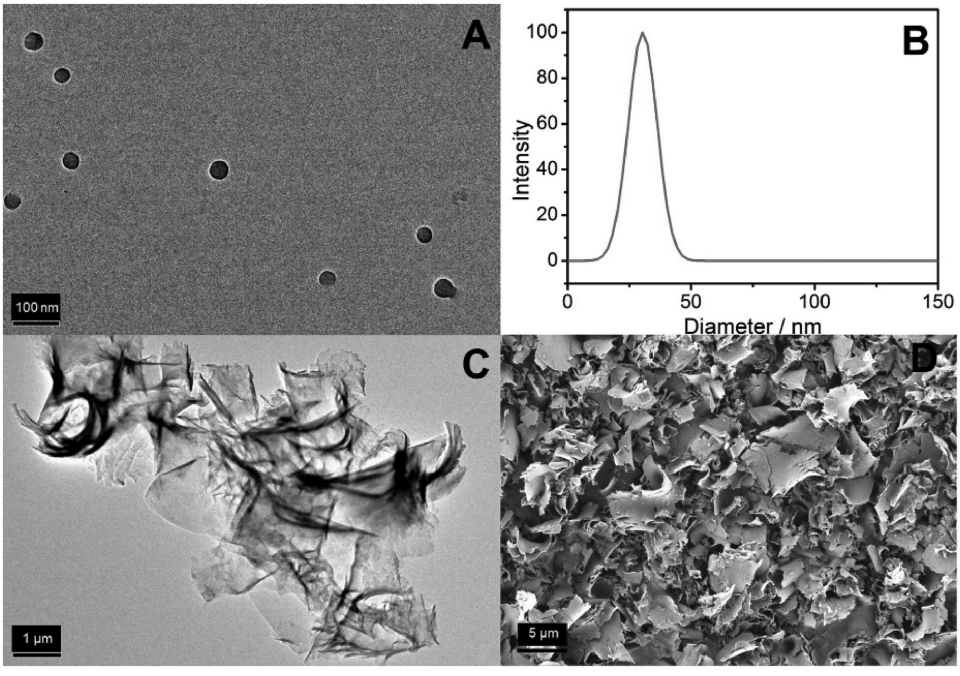

Figure 2. Morphological features. A) TEM images and B) diameter distributions of **$Eu(TTA)_3$tpy-mim_2** in neat water at a concentration of 0.5 mmol L^{-1}. C) TEM and D) SEM images of supramolecular hydrogels. Laponite/ASAP/**$Eu(TTA)_3$tpy-mim_2** = 2.9/0.087/0.077 wt%.

Adv. Funct. Mater. **2016**,
DOI: 10.1002/adfm.201604379

Supporting Information). In contrast, the luminescence decay rate of **Eu(TTA)$_3$tpy-mim$_2$** in H_2O only decreased slightly compared to that in D_2O, leading to a small coordinated water number of 0.07 in the first coordination sphere of Eu^{3+} ions in **Eu(TTA)$_3$tpy-mim$_2$** complexes. Our results confirm that synergistically coordinating TTA and terpyridine moieties with Eu^{3+} ions, in combination with the hydrophobic microenvironment in the spherical micelles, results in decrease of the water number in the first coordination sphere of Eu^{3+} ions significantly, thus retaining the strong luminescence of **Eu(TTA)$_3$tpy-mim$_2$** complexes in water.

Mixing **Eu(TTA)$_3$tpy-mim$_2$** solution with ASAP exfoliated Laponite nanosheets in neat water led to formation of luminescent hydrogels, which can be molded into free-standing objects easily (Figure 1C(ii) and Figure 4). The composition of organic and water components in the hydrogels was determined to be 0.16% and 97%, respectively. The high water content in the resulting hydrogels renders their feature analogues to aqua materials. However, mixing $Eu(TTA)_3$ or $Eu(TTA)_3$tpy water suspension with ASAP exfoliated Laponite nanosheets did not result in gelation (Figure S16, Supporting Information). Moreover, the presence of ASAP quenched the luminescence of Eu^{3+} dramatically, implying the existence of competitive coordination of ASAP with Eu^{3+} ions (Figure S16c,d, Supporting Information). In addition, adding of a 1-hexyl-3-methylimidazolium bromide (C_6mim) (Scheme 2) (2 molar equivalents to **Eu(TTA)$_3$tpy-mim$_2$**) into the supramolecular hydrogels (Figure 1C(iii)) gave rise to the gel-sol transition, due to the competitive electrostatic interaction between the imidazole salt and ASAP exfoliated Laponite nanosheet (Figure 1C(iv)). These results suggest that the micelles interact with Laponite nanosheets via electrostatic interactions. Overall, our results indicate that the gelation proceeds following a hierarchically self-assembling process. Initially, **Eu(TTA)$_3$tpy-mim$_2$** spontaneously aggregates into spherical micelles coated with positively charged imidazole units in water. The micelles subsequently serve as the binders and undergo coassembly with the ASAP exfoliated Laponite nanosheets into the hierarchical supramolecular hydrogels, driven by the electrostatic interactions between the positively charged imidazoles and the negatively charged Laponite nanosheets. Moreover, the zeta potential of the pristine Laponite nanosheets was measured as −37.5 mV (Figure S17a, Supporting Information), and the zeta potential of the ASAP exfoliated Laponite nanosheets underwent a further negative shift to −54.6 mV (Figure S17b, Supporting Information), indicating that ASAP is wrapped at their positive-charged edge parts.[8a] Accordingly, these negatively charged Laponite nanosheets would facilitate the attraction of positive charge.

We characterized the morphological feature of the supramolecular hydrogels by TEM and SEM (Figure 2C,D). In great contrast to the spherical micelles formed by **Eu(TTA)$_3$tpy-mim$_2$** alone, we observed 2D nanoflakes in micrometer size by TEM in the supramolecular hydrogels, where the Laponite nanosheets were homogenously dispersed. This morphology was confirmed by SEM, which clearly showed flat flakes in the dried hydrogels. The dried and ground xerogels were also characterized by powder X-ray diffraction; the broad diffraction pattern of pristine Laponite at $\approx 2\theta = 6.96°$ implies that the interlayer space in pristine Laponite is ≈1.3 nm (Figure S18a, Supporting Information), which is in good agreement with the reported value.[17] The addition of ASAP does not affect the interlayer space of the Laponite nanosheet (Figure S18b, Supporting Information); this phenomenon further confirmed that ASAP is site-specific wrapped at their positive-charged edge parts, but not located at the interlayer of Laponite. However, after introducing **Eu(TTA)$_3$tpy-mim$_2$**, the broad peak shifted to $2\theta = 4.94°$, revealing a 1.8 nm interlayer space (Figure S18c, Supporting Information). The enlarged Laponite interlayer space in supramolecular xerogels confirmed **Eu(TTA)$_3$tpy-mim$_2$** located in between the interlayer space of Laponite.[18] These results demonstrate that the spherical micelles self-assemble with ASAP exfoliated Laponite nanosheets into high dimensional networks.

We investigated the photoluminescent property of the supramolecular hydrogels and the mixture of $Eu(TTA)_3$tpy or $Eu(TTA)_3$ water suspension and ASAP exfoliated Laponite nanosheets. Although $Eu(TTA)_3$tpy and **Eu(TTA)$_3$tpy-mim$_2$** exhibited comparable luminescence in the solid state, only the supramolecular hydrogel (the red line in Figure 1D, Figure 1C(iii)) showed a strong luminescence, while the luminescence of the mixture of $Eu(TTA)_3$tpy (the blue line in Figure 1D) or $Eu(TTA)_3$ (the black line in Figure 1D) water suspension and ASAP exfoliated Laponite nanosheets containing a same Eu^{3+} concentration with the hydrogel was quenched significantly. In addition, the luminescence lifetime and quantum efficiency of Eu^{3+} ions in the supramolecular hydrogels are comparable to those of **Eu(TTA)$_3$tpy-mim$_2$** solution. However, mixing $Eu(TTA)_3$ or $Eu(TTA)_3$tpy water suspension with ASAP exfoliated Laponite nanosheets led to a dramatic decrease of the luminescence lifetime and quantum efficiency of Eu^{3+} ions compared to those of the related water suspension alone (Table S1, Supporting Information). These results clearly suggest that the luminescence of Eu^{3+} complexes in the supramolecular hydrogels can be retained following the addition of the ASAP exfoliated Laponite nanosheets.

To reveal the reason for the luminescence difference variation of the samples involving ASAP exfoliated Laponite nanosheets, and to verify the existence of competitive coordination of ASAP with Eu^{3+} ions, we prepared the supramolecular hydrogel and the mixture $Eu(TTA)_3$ or $Eu(TTA)_3$tpy D_2O suspension with ASAP exfoliated Laponite nanosheets in D_2O medium. The luminescence lifetime and quantum efficiency of Eu^{3+} ions in the physical mixtures decreased dramatically compared to that of the powder $Eu(TTA)_3$ and $Eu(TTA)_3$tpy dispersed in D_2O. This can be attributed to the competitive complexation of acrylate on ASAP with Eu^{3+} ions. Meanwhile, the presence of ASAP did not affect the luminescence lifetime and quantum efficiency of Eu^{3+} ions in the supramolecular hydrogel using D_2O as the media (Table 1 and Table S1 (Supporting Information)). These results confirm the collaborative protection effect of the spherical micelles and synergistic coordination of Eu^{3+} in the supramolecular hydrogels. The synergistic chelating of terpyridine and TTA units, in combination with the hydrophobic microenvironment for Eu^{3+} ions, can not only prevent the infiltration of water molecules but also shield the lanthanide emitting center from the competitive coordination with acrylate units on ASAP.

We carried out rheological experiments to estimate the mechanical properties of the supramolecular hydrogels (**Figure 3**). The storage modulus (G') value was larger than the loss modulus (G'') value over a wide frequency range (ω = 0.05–100 rad s^{-1}), indicating the characteristic of a stable gel-phase material, indicating the hydrogelation of the micelles and ASAP exfoliated Laponite nanosheets in water. In addition, the moduli of the hydrogels is only slightly dependent to the applied angular frequency (Figure 3A). Note that the G' value of our hydrogels reaches 11 KPa, which is comparable to the Laponite-containing hydrogels utilizing dendrimers as the binders, and an order of magnitude larger compared to that of traditional supramolecular hydrogels.[19] The corresponding strain sweeps for the supramolecular hydrogels are shown in Figure 3B, at fixed strain amplitude sweep, the storage modulus remains constant until the yield strain is reached at the critical strain region (γ = 31.7%), implying the destruction of the gel network and a gel-to-quasi-liquid state transition. This γ value is larger than the reported Laponite nanoclay supramolecular hydrogels, verifying that our supramolecular hydrogels possess better damage resistance ability compared to the reported Laponite nanoclay supramolecular hydrogels.[8a,10a] We also tested the recovery property of the supramolecular hydrogel by employing alternating strain amplitudes of 100% and 0.1% at a fixed frequency (1.0 Hz). As shown in Figure 3C, the supramolecular hydrogel behaves as a liquid and solid alternately (30 s) with a quick recovery to the original values of the moduli in the two regimes.

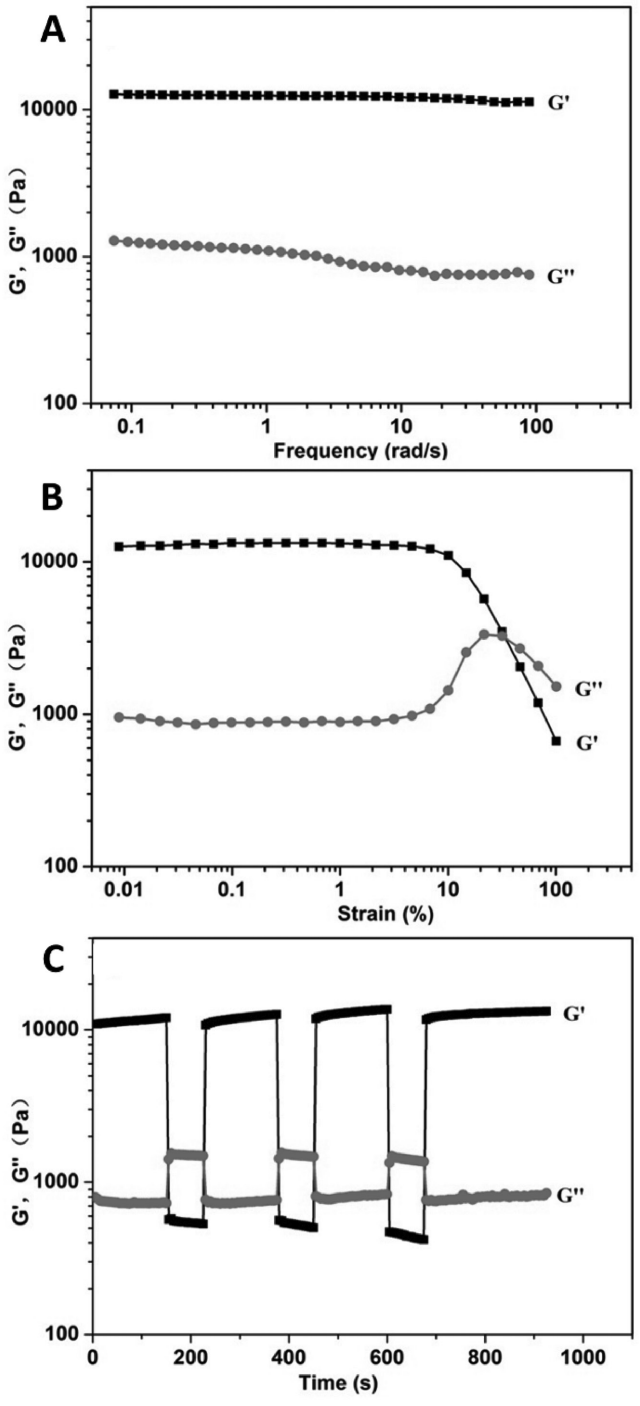

Figure 3. Rheological properties. A) Frequency (ω) sweep tests at ω = 0.05–100 rad s^{-1} and strain (γ) = 0.5% of the supramolecular hydrogels at 25 °C; B) strain sweep tests at γ = 0.05%–100% with ω = 6.28 rad s^{-1}; C) continuous step strain tests at γ = 0.1% and 100%.

In addition, we characterized the thermal stability of our supramolecular hydrogels. We also determined the rheological properties of our supramolecular hydrogels at 70 °C (Figure S19, Supporting Information). No obvious change was observed in both G' and G'' values compared to room temperature, indicating that the mechanical properties of the hydrogels once formed hardly depend on the temperature. In addition, supramolecular hydrogels did not show thermal-induced phase transition until heating to 70 °C (Figure S20, Supporting Information), suggesting an excellent thermal stability for the hydrogels. It is worth noting that the heating–cooling process does not affect the luminescent properties of the supramolecular hydrogels. These results demonstrate that coassembly of the spherical micelles formed amphiphilic monomer **$Eu(TTA)_3$tpy-mim_2** and exfoliated Laponite nanosheets allow for creating a robust hydrogel with strong luminescence in water.

Based on the rheological study, we demonstrated the self-healing ability of the supramolecular hydrogel by cutting a disk-shaped hydrogel into two half pieces by using a razor (**Figure 4**). The two closely placed pieces rapidly recombined into one entire piece, which is strong enough to be lifted up under shaking in 1 min (see Video S1 in the Supporting Information). After aging for 1 h, the crack in the reproduced hydrogel disappeared completely, leading to a healed hydrogel. It remains a daunting challenge to achieve fast and efficient healing for tough hydrogels,[20] which usually happened in soft host–guest supramolecular hydrogels.[19a] However, our supramolecular hydrogels are not only mechanically tough but also have a fast-recovery capability. The mechanical properties originate largely from the toughness of Laponite nanosheets and the self-healing ability result from the hierarchical self-assembly strategy. Our study demonstrates that organic–inorganic hierarchical self-assembly is a versatile and effective strategy to readily create self-healable luminescent hydrogels with high mechanical strength and extraordinary photophysical property. Our hydrogels utilize the relatively cheap Ln complexes with large Stokes shifts, sharp and tunable emission profiles, and

DOI: 10.1002/adfm.201604379

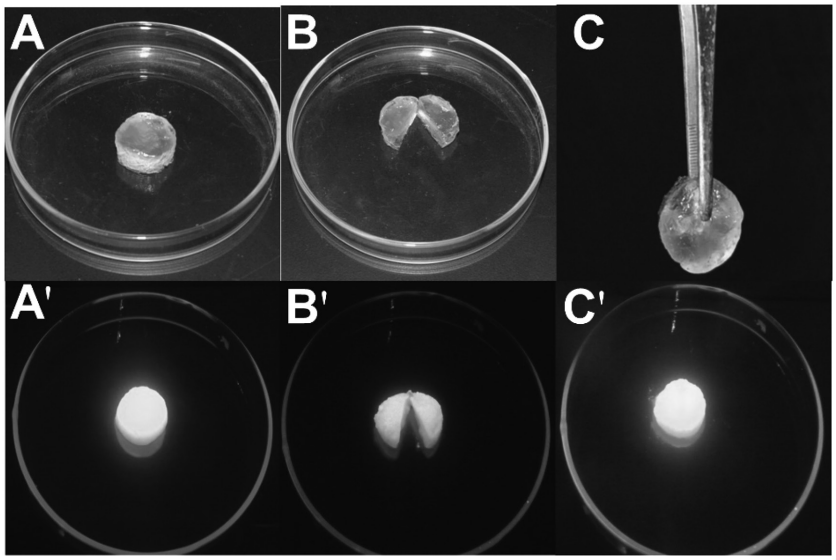

Figure 4. Self-healing experiments of the organic–inorganic hybrid hydrogels. A) Original hydrogels Laponite/ASAP/**Eu(TTA)$_3$tpy-mim$_2$** = 2.9/0.087/0.077 wt% ([**Eu(TTA)$_3$tpy-mim$_2$**] = 0.5 mmol L^{-1}), Pictures B) before and C) after adhesion freshly cut surfaces at 25 °C; A′) Original hydrogels, Pictures B′) before and C′) after adhesion freshly cut surfaces under 365 nm UV lamp illumination. The diameter of the petri dish is 9 cm.

long-lived excited states as the emitting source, thus rendering them broadly applicable for fabrication of many devices.

3. Conclusion

In summary, we have reported on robust luminescent hydrogels using lanthanide complexes as emitting sources via a hierarchical organic–inorganic self-assembling strategy. A new organic ligand consisting of a terpyridine unit and two flexibly linked methylimidazole moieties has been designed and synthesized to coordinate with Eu(TTA)$_3$, yielding a stable amphiphilic Eu^{3+}-containing monomer. Due to the synergistic coordination of TTA and terpyridine units, the monomer forms spherical micelles in water, thus maintaining the luminescence of Ln complexes in water. The micelles further coassemble with exfoliated Laponite nanosheets coated with sodium polyacrylate into networks based on the electrostatic interactions, resulting in the supramolecular hydrogel. Our results indicate that the strong luminescence of Eu^{3+} ions can be retained in hydrogels containing ASAP. Incorporation of inorganic Laponite nanosheets allows for improvement of the mechanical property of the supramolecular hydrogel substantially. Our study demonstrates that the hierarchical self-assembly is a versatile and effective strategy to readily create self-healable luminescent hydrogels with high mechanical strength and extraordinary photophysical property.

4. Experimental Section

Materials: All chemicals were commercially available unless noted otherwise. 2-thenoyltrifluoroacetate (TTA) was purchased from Aldrich and used as received. The layered clay (Laponite XLG), was purchased from Rockwood Additives Ltd and was used as received without further purification.

Measurements: Rheological tests of hydrogels were carried out by using an Anton Paar model MCR-301 rheometer, with a 25 mm diameter parallel plate attached to a transducer. The gap was set at 1.0 mm. TEM experiments were performed using a Tecnai 20 high resolution transmission electron microscope operating at an accelerating voltage of 200 keV. The sample for TEM measurements was prepared by smearing the hydrogel onto a copper grid. The grid was then air-dried and imaged. SEM images were recorded on a Hitachi S-3500N scanning electron microscope. The sample for SEM measurements was prepared as follows: the dried xerogel was first ground to powder, and then the powder was dispersed onto a coverslip. The sample solution for DLS measurements was prepared by filtering the solution through a 450 nm Millipore filter into a clean scintillation vial. The samples were examined on a laser light scattering spectrometer (BI-200SM) equipped with a digital correlator (TurboCorr) at 532 nm at a scattering angle of 90°. The hydrodynamic radius (R_h) was determined by dynamic light scattering experiments, and the radius of gyration (R_g) was obtained from static light scattering data at different scattering angles. The steady-state luminescence spectra were measured on an Edinburgh Instruments FS920P near-infrared spectrometer, with a 450 W xenon lamp as the steady-state excitation source, a double excitation monochromator (1800 lines mm^{-1}), an emission monochromator (600 lines mm^{-1}), a semiconductor-cooled Hamamatsu RMP928 photomultiplier tube.

Preparation of Supramolecular Hydrogel: Laponite XLG (150 mg) was suspended in 3.5 mL water and stirred for 10 min at room temperature, and an aqueous solution of ASAP (4.5 mg, 0.5 mL) was added to the resulting suspension. After stirring for 10 min, an aqueous solution of **Eu(TTA)$_3$tpy-mim$_2$** (4.0 mg, 1.0 mL) was added, and then the mixture was stirred for 3 min and then allowed to self-standing.

*Preparation of **Eu(TTA)$_3$tpy-mim$_2$***: Tepy-mim$_2$ (415 mg, 0.5 mmol) and Eu(TTA)$_3$ (408 mg, 0.5 mmol) were suspended in MeOH (10 mL). The reaction mixture was heated to 80 °C for 4 h and poured into 100 mL ether. The precipitate was collected by filtration, washed with ether, and dried, and final product was obtained in 90% yield. ^{1}H NMR (400 MHz, Deuterated dimethyl sulfoxide (DMSO-d6), ppm) δ 9.13 (s, 2H), 8.76 (d, J = 4.7 Hz, 2H), 8.68 (d, J = 7.9 Hz, 2H), 8.64 (s, 2H), 8.06 (td, J = 7.8, 1.7 Hz, 2H), 7.78 (d, J = 7.2 Hz, 2H), 7.71 (d, J = 1.6 Hz, 2H), 7.55 (dd, J = 6.9, 5.3 Hz, 2H), 7.37 (m, 3H), 6.96 (d, J = 2.0 Hz, 2H), 6.63 (s, 1H), 6.46 (s, 3H), 6.35 (s, 3H), 4.49 (s, 3H), 4.18 (t, J = 7.1 Hz, 4H), 4.08 (t, J = 6.3 Hz, 4H), 3.84 (s, 6H), 1.83 (m, 4H), 1.75 (m, 4H), 1.49 (m, 4H), 1.34 (m, 4H). Matrix Laster Desorption Time of Flight Mass Spectrometry (MALDI-MS) [M-2Br]$^+$ calcd for $C_{65}H_{60}EuF_9N_7O_8S_3^+$ 1486.2734; found: 1486.2665; Anal Calcd for $C_{65}H_{60}Br_2EuF_9N_7O_8S_3$: C, 47.43; H, 3.67; N, 5.96; Found: C, 47.29; H, 3.72; N, 5.75.

Supporting Information

Supporting Information is available from the Wiley Online Library or from the author.

Acknowledgements

This work was financially supported by the National Natural Science Foundation of China (21171046, 21502039, 21271060), the Natural Science Foundation of Hebei Province (Nos. B2016202149,

B2016202147), the Educational Committee of Hebei Province (LJRC021, QN2015172).

Received: August 24, 2016
Revised: September 30, 2016
Published online:

[1] a) L. Maggini, D. Bonifazi, *Chem. Soc. Rev.* **2012**, *41*, 211; b) Y. Cui, Y. Yue, G. Qian, B. Chen, *Chem. Rev.* **2011**, *112*, 1126; c) M. Burnworth, L. Tang, J. R. Kumpfer, A. J. Duncan, F. L. Beyer, G. L. Fiore, S. J. Rowan, C. Weder, *Nature* **2011**, *472*, 334; d) N. N. Katia, A. Lecointre, M. N. Regueiro-Figueroa, C. Platas-Iglesias, L. C. J. Charbonnière, *J. Inorg. Chem.* **2011**, *50*, 1689.

[2] a) S. V. Eliseeva, J.-C. G. Bünzli, *Chem. Soc. Rev.* **2010**, *39*, 189; b) J. Rocha, L. D. Carlos, F. A. A. Paz, D. Ananias, *Chem. Soc. Rev.* **2011**, *40*, 926; c) M. C. Heffern, L. M. Matosziuk, T. J. Meade, *Chem. Rev.* **2013**, *114*, 4496; d) J.-C. G. Bünzli, C. Piguet, *Chem. Soc. Rev.* **2005**, *34*, 1048.

[3] a) L. D. Carlos, R. A. Ferreira, V. de Zea Bermudez, B. Julian-Lopez, P. Escribano, *Chem. Soc. Rev.* **2011**, *40*, 536; b) K. Binnemans, *Chem. Rev.* **2009**, *109*, 4283; c) S. Tang, A. Babai, A. V. Mudring, *Angew. Chem., Int. Ed.* **2008**, *47*, 7631; d) A. V. Mudring, S. Tang, *Eur. J. Inorg. Chem.* **2010**, *2010*, 2569; e) M. P. Jensen, J. Neuefeind, J. V. Beitz, S. Skanthakumar, L. Soderholm, *J. Am. Chem. Soc.* **2003**, *125*, 15466.

[4] a) K. S. Toohey, N. R. Sottos, J. A. Lewis, J. S. Moore, S. R. White, *Nat. Mater.* **2007**, *6*, 581; b) J. Feng, H. Zhang, *Chem. Soc. Rev.* **2013**, *42*, 387; c) P. Li, Y. Wang, H. Li, G. Calzaferri, *Angew. Chem., Int. Ed.* **2014**, *53*, 2904; d) L. E. Buerkle, S. J. Rowan, *Chem. Soc. Rev.* **2012**, *41*, 6089; e) G. Calzaferri, S. Huber, H. Maas, C. Minkowski, *Angew. Chem.* **2003**, *115*, 3860; *Angew. Chem., Int. Ed.* **2003**, *42*, 3732; f) Z. Popović, M. Otter, G. Calzaferri, L. De Cola, *Angew. Chem.* **2007**, *119*, 6301; *Angew. Chem., Int. Ed.* **2007**, *46*, 6188; g) H. Maas, G. Calzaferri, *Angew. Chem.* **2002**, *114*, 2389; *Angew. Chem., Int. Ed.* **2002**, *41*, 2284.

[5] a) S. Petoud, S. M. Cohen, J.-C. G. Bünzli, K. N. Raymond, *J. Am. Chem. Soc.* **2003**, *125*, 13324; b) A. de Bettencourt-Dias, P. S. Barber, S. Bauer, *J. Am. Chem. Soc.* **2012**, *134*, 6987; c) J. Xu, T. M. Corneillie, E. G. Moore, G.-L. Law, N. G. Butlin, K. N. Raymond, *J. Am. Chem. Soc.* **2011**, *133*, 19900.

[6] a) A. Harada, R. Kobayashi, Y. Takashima, A. Hashidzume, H. Yamaguchi, *Nat. Chem.* **2011**, *3*, 34; b) T. Aida, E. Meijer, S. Stupp, *Science* **2012**, *335*, 813; c) A.-J. Avestro, M. E. Belowich, J. F. Stoddart, *Chem. Soc. Rev.* **2012**, *41*, 5881; d) M. Yamanaka, K. Yanai, Y. Zama, J. Tsuchiyagaito, M. Yoshida, A. Ishii, M. Hasegawa, *Chem. - Asian J.* **2015**, *10*, 1299; e) A. B. Ihsan, T. L. Sun, S. Kuroda, M. A. Haque, T. Kurokawa, T. Nakajima, J. P. Gong, *J. Mater. Chem. B* **2013**, *1*, 4555.

[7] a) Y. Chen, Y. Liu, *Adv. Mater.* **2015**, *27*, 5403; b) P. Wei, X. Yan, F. Huang, *Chem. Soc. Rev.* **2015**, *44*, 815; c) G. Yu, X. Yan, C. Han, F. Huang, *Chem. Soc. Rev.* **2013**, *42*, 6697; d) M. Nakahata, Y. Takashima, H. Yamaguchi, A. Harada, *Nat. Commun.* **2011**, *2*, 511; e) T. L. Sun, T. Kurokawa, S. Kuroda, A. B. Ihsan, T. Akasaki, K. Sato, M. A. Haque, T. Nakajima, J. P. Gong, *Nat. Mater.* **2013**, *12*, 932; f) H. J. Zhang, T. L. Sun, A. K. Zhang, Y. Ikura, T. Nakajima, T. Nonoyama, T. Kurokawa, O. Ito, H. Ishitobi, J. P. Gong, *Adv. Mater.* **2016**, *28*, 4884.

[8] a) Q. Wang, J. L. Mynar, M. Yoshida, E. Lee, M. Lee, K. Okuro, K. Kinbara, T. Aida, *Nature* **2010**, *463*, 339; b) K. Haraguchi, T. Takehisa, *Adv. Mater.* **2002**, *14*, 1120.

[9] In our previous work, we presented a two-step strategy to prepare lanthanide-based red-light emitting hybrid materials by first exchanging counter Na^+ of Laponite by Eu^{3+} and subsequently in situ forming Eu^{3+}–*β*-diketonate complexes on Laponite platelets by addition of 2-thenoyltrifluoroacetate ligand. However, the counter Na^+ is essential for the exfoliation behavior of Laponite in water, after the ion exchange process, the Eu^{3+} loaded Laponite cannot be delaminated to individual disks anymore and only aqueous suspension was obtained. In addition, the presence of ASAP leads to nearly completely luminescent quenching, which is attributed to the competitive complexation of acrylate to Eu^{3+}. For details, please see: D. Yang, Y. Wang, Y. Wang, Z. Li, H. Li, *ACS Appl. Mater. Interfaces* **2015**, *7*, 2097.

[10] a) S. Tamesue, M. Ohtani, K. Yamada, Y. Ishida, J. M. Spruell, N. A. Lynd, C. J. Hawker, T. Aida, *J. Am. Chem. Soc.* **2013**, *135*, 15650; b) K. Haraguchi, R. Farnworth, A. Ohbayashi, T. Takehisa, *Macromolecules* **2003**, *36*, 5732.

[11] F.-F. Chen, H.-B. Wei, Z.-Q. Bian, Z.-W. Liu, E. Ma, Z.-N. Chen, C.-H. Huang, *Organometallics* **2014**, *33*, 3275.

[12] a) Z. Li, P. Li, Q. Xu, H. Li, *Chem. Commun.* **2015**, *51*, 10644; b) Z. Li, Z. Hou, D. Ha, H. Li, *Chem. - Asian J.* **2015**, *10*, 2720.

[13] a) X.-L. Li, L.-X. Shi, L.-Y. Zhang, H.-M. Wen, Z.-N. Chen, *Inorg. Chem.* **2007**, *46*, 10892; b) H. Li, N. Lin, Y. Wang, Y. Feng, Q. Gan, H. Zhang, Q. Dong, Y. Chen, *Eur. J. Inorg. Chem.* **2009**, *2009*, 519; c) Z. Li, J. Wang, M. Chen, Y. Wang, *Chem. - Asian J.* **2016**, *11*, 745.

[14] a) Y. He, Z. Li, P. Simone, T. P. Lodge, *J. Am. Chem. Soc* **2006**, *128*, 2745; b) F. Chécot, S. Lecommandoux, Y. Gnanou, H. A. Klok, *Angew. Chem., Int. Ed.* **2002**, *41*, 1339.

[15] a) R. M. Supkowski, W. D. Horrocks, *Inorg. Chem.* **1999**, *38*, 5616; b) I. Clarkson, R. Dickins, A. de Sousa, *J. Chem. Soc., Perkin Trans. 2* **1999**, 493; c) R. M. Supkowski, W. D. Horrocks, *Inorg. Chim. Acta* **2002**, *340*, 44.

[16] a) J. Liu, M.-A. Morikawa, N. Kimizuka, *J. Am. Chem. Soc.* **2011**, *133*, 17370; b) M.-A. Morikawa, S. Tsunofuri, N. Kimizuka, *Langmuir* **2013**, *29*, 12930.

[17] a) M. M. Lezhnina, T. Grewe, H. Stoehr, U. Kynast, *Angew. Chem., Int. Ed.* **2012**, *51*, 10652; *Angew. Chem.* **2012**, *124*, 10805; b) B. V. Lotsch, G. A. Ozin, *ACS Nano* **2008**, *2*, 2065.

[18] a) Y. Yao, Z. Li, H. Li, *RSC Adv.* **2015**, *5*, 70868; b) Q. Xu, Z. Li, Y. Wang, H. Li, *Photochem. Photobiol. Sci.* **2016**, *15*, 405.

[19] a) H. Chen, X. Ma, S. Wu, H. Tian, *Angew. Chem., Int. Ed.* **2014**, *53*, 14149; b) X. Yan, D. Xu, X. Chi, J. Chen, S. Dong, X. Ding, Y. Yu, F. Huang, *Adv. Mater.* **2012**, *24*, 362; c) S. Dong, Y. Luo, X. Yan, B. Zheng, X. Ding, Y. Yu, Z. Ma, Q. Zhao, F. Huang, *Angew. Chem.* **2011**, *50*, 1905; *Angew. Chem., Int. Ed.* **2011**, *123*, 1945.

[20] S. Hou, P. X. Ma, *Chem. Mater.* **2015**, *27*, 7627.